Kinetics of the Separately Observable Formation and Decomposition of the Intermediate Complex in Aromatic Nucleophilic Substitution. Reactions of 2,4-Dinitro-1-naphthyl Ethyl Ether with *n*-Butyl- and *t*-Butylamine in Dimethyl Sulfoxide Solution[1]

Jon A. Orvik and J. F. Bunnett

Contribution from the University of California, Santa Cruz, California 95060.
Received September 2, 1969

Abstract: The reactions named in the title, which form the respective 2,4-dinitro-1-naphthylbutylamines (**8**), occur in two distinct stages. The spectrum of an intermediate develops at a rate which is measurable in a stopped-flow apparatus, and then decays at a slower and easily measurable rate. The kinetics of both stage I and stage II have been studied, and equilibrium constants have been determined for the stage I equilibrium and the acid–base equilibrium between product **8** and its conjugate base **9**. The evidence indicates that the observable intermediate is the conjugate base (**7**) of the initial σ complex (**6**). Formation of the intermediate is not base catalyzed. Its transformation to product **8** is first order in butylammonium ion but independent of amine concentration. The mechanism of base catalysis of the overall reaction is thereby indicated to be general acid catalysis of leaving group expulsion from the conjugate base of the σ-complex intermediate.

Steady-state kinetics have both strengths and limitations as evidence of reaction mechanism. In the case of aromatic nucleophilic substitution reactions involving amine reagents, an important conclusion that has emerged from steady-state kinetic studies is that these reactions proceed *via* a metastable intermediate. For the familiar reactions of amines with 1-substituted 2,4-dinitrobenzenes (**1**), the intermediate is usually represented as **2**.

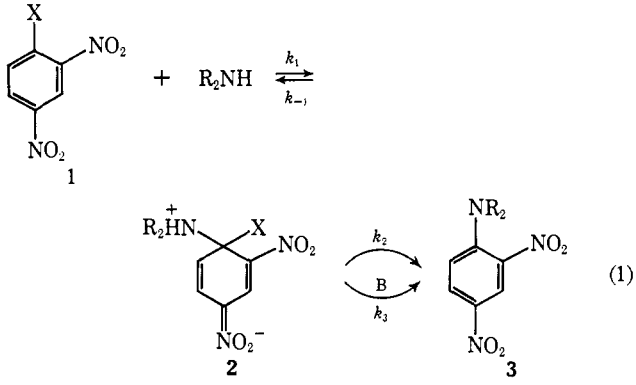

(1)

Much of the evidence concerns the susceptibility of some but not all of these reactions to catalysis by bases, such as NaOH or amines.[2-4] Salient facts are that the incidence of base catalysis is related to how good the leaving group is, being greater with worse leaving groups, that in favorable cases reactions are base catalyzed at low but not at high base concentrations, that *general* base catalysis obtains, and that in one such case the magnitude of the heavy atom isotope effect (with respect to the isotope in the first atom of the leaving group) diminishes with increasing base concentration.[5] These show that the first step of reaction 1 is not base catalyzed whereas the second step is.

However, it has not been possible from steady-state kinetics to elucidate in detail how a base catalyzes the expulsion of leaving group X from intermediate **2**. Also, there has been no direct experimental evidence as to whether the low steady-state concentration of the intermediate represents mainly the σ complex of amine with substrate (*e.g.*, **2**) or the conjugate base of that σ complex (*e.g.*, **4**).

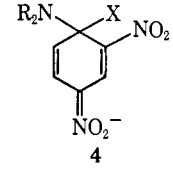

Three principal mechanisms for base catalysis of leaving group expulsion from **2** have been suggested.

(a) Rate-limiting proton transfer from **2** to base, forming **4** from which X is then rapidly expelled. This interpretation was suggested in 1958,[2a] but was disfavored in subsequent discussions,[2b,c,3,6] and is shown to be untenable for at least one case by the fact that base-catalyzed expulsion of the phenoxy leaving group is slower when the ether oxygen is the isotope of mass 18.[5]

(b) Concerted rupture of the N–H and C–X bonds of **2**, provoked by attack of base on H. This E2-like process was also suggested in 1958,[2a] has been disfavored in some subsequent discussions,[2b,c,3] but is advocated in a recent review.[6]

(c) Reversible reaction of intermediate **2** with base (B), to form the conjugate base intermediate (**4**) and the conjugate acid of the base (BH) (step 2a), followed

(1) This investigation was supported in part by Public Health Service Research Grant No. GM 14647 from the National Institute of General Medical Sciences.

(2) (a) J. F. Bunnett and J. J. Randall, *J. Amer. Chem. Soc.*, **80**, 6020 (1958); (b) J. F. Bunnett and R. H. Garst, *ibid.*, **87**, 3879 (1965); (c) J. F. Bunnett and C. Bernasconi, *ibid.*, **87**, 5209 (1965); (d) J. F. Bunnett and R. H. Garst, *J Org. Chem.*, **33**, 2320 (1968).

(3) A. J. Kirby and W. P. Jencks, *J. Amer. Chem. Soc.*, **87**, 3217 (1965).

(4) C. F. Bernasconi, *J. Org. Chem.*, **32**, 2947 (1967).

(5) C. R. Hart and A. N. Bourns, *Tetrahedron Lett.*, 2995 (1966).

(6) E. Buncel, A. R. Norris, and K. E. Russell, *Quart. Rev.* (London), **22**, 123 (1968).

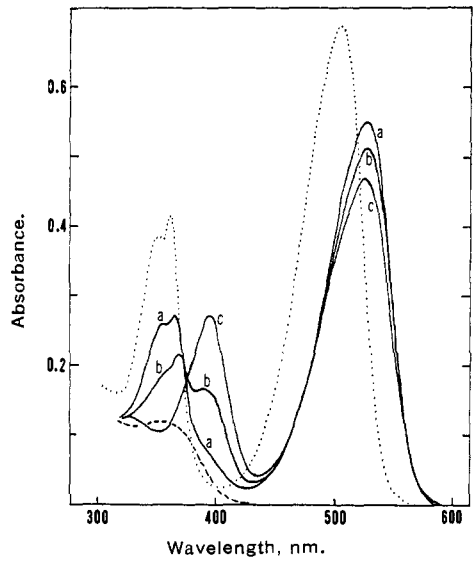

Figure 1. Spectra relevant to reaction of **5** with *n*-butylamine, all in DMSO solution: dashed line (- - -), **5** before addition of amine; curves a, b, and c, *ca.* 5, 18, and 144 min, respectively, after addition of 0.081 *M n*-butylamine; dotted line (· · ·), Jackson–Meisenheimer addition product of $NaOCH_3$ to methyl 2,4-dinitro-1-naphthyl ether.

by rate-limiting expulsion of X from **4** with general acid catalysis by BH (step 2b). This interpretation was first proposed in 1960,[7] and has been favored in

$$2 + B \underset{}{\overset{\text{fast}}{\rightleftharpoons}} 4 + BH \qquad (2a)$$

$$4 + BH \longrightarrow \left[\begin{array}{c} R_2N \quad X\cdots H\cdots B \\ \quad\quad\quad\quad NO_2 \\ \quad\quad\quad\quad\quad\quad NO_2 \end{array}\right] \longrightarrow 3 \qquad (2b)$$

transition state

the majority of recent discussions. It calls for the same overall rate law irrespective of whether the intermediate is largely present as the initial σ complex (**2**) or as its conjugate base (**4**), providing that equilibrium reaction 2a is rapid compared to reactions of decomposition of **2** or **4**.[2c,d] In contrast, interpretation (a) would be impossible and (b) illogical if the intermediate were shown to occur mainly as **4**. The question of logic is discussed below.

We have discovered that the reaction of 2,4-dinitro-1-naphthyl ethyl ether (**5**) with primary aliphatic amines in dimethyl sulfoxide (DMSO) solution occurs in two separately observable stages. A systematic investigation of the kinetics and equilibria of this system has enabled questions to be answered that could not be answered from steady-state kinetics, as well as verification of conclusions already drawn. Moreover, the data enable construction of a quantitative energy profile for the reaction.

Our observations will be shown to be consistent with the mechanism of Scheme I.

(7) J. F. Bunnett and G. T. Davis, *J. Amer. Chem. Soc.*, **82**, 665 (1960), footnote 27.

Scheme I

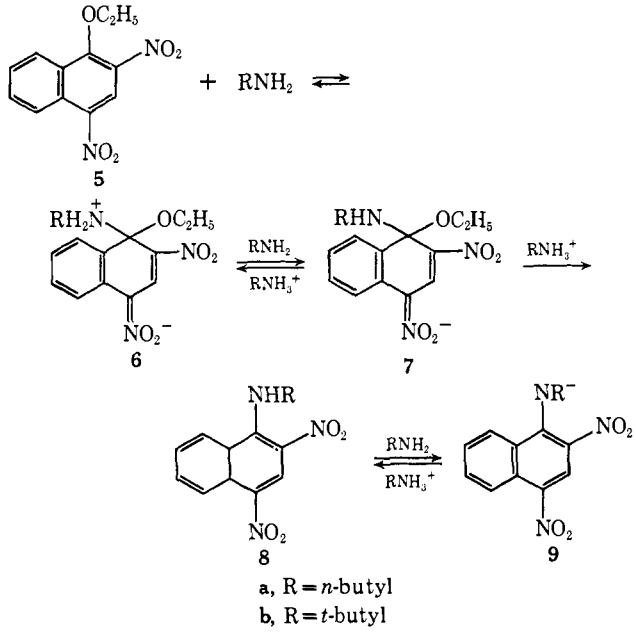

a, R = *n*-butyl
b, R = *t*-butyl

Results

General Features. The reaction of *n*-butylamine with DNN[8] ethyl ether (**5**) in DMSO at room temperature produces, ultimately, a quantitative yield of 2,4-DNN *n*-butylamine, **8**a. The reaction takes place in two distinct stages, recognizable by two spectral changes. The first spectral change (from the low, dashed curve to curve a, Figure 1) occurs immediately upon addition of *n*-butylamine to a DMSO solution of **5**. Its rate is too fast to measure by conventional means but is measurable by a spectrophotometric stopped-flow method. The second spectral change (from curve a to curve c, Figure 1) is much slower. The chemical transformations responsible for the first and second spectral changes are termed stage I and stage II, respectively.

The final isolable product is 2,4-DNN *n*-butylamine (**8**a), but curve c, which represents the spectrum of the infinity solution for the overall reaction, obviously is not the spectrum of **8**a. A solution of **8**a in DMSO has a single absorption maximum in the visible region at 410 nm. Nmr experiments show that in the presence of *n*-butylamine the product **8**a is in rapid equilibrium with its conjugate base, anion **9**a. Under the experimental conditions for Figure 1, this equilibrium lies entirely on the side of the anion. Curve c therefore represents the spectrum of **9**a.

The striking similarity of curve a in Figure 1 to the spectrum of the Jackson–Meisenheimer complex of $NaOCH_3$ with DNN methyl ether (Figure 1, dotted curve)[9] and the general resemblance to spectra of other similar complexes for which there is adequate evidence of structure[10,11] serve to identify curve a as being due to σ-complex intermediate **6**a or its conjugate base,

(8) DNN symbolizes the 2,4-dinitro-1-naphthyl group.
(9) This work; Fendler, *et al.*,[10] report the spectrum of the addition complex in methanol.
(10) J. H. Fendler, E. J. Fendler, W. E. Byrne, and C. E. Griffin, *J. Org. Chem.*, **33**, 977 (1968).
(11) (a) R. Foster and C. A. Fyfe, *Rev. Pure Appl. Chem.*, **16**, 61 (1966); (b) W. E. Byrne, E. J. Fendler, J. H. Fendler, and C. E. Griffin, *J. Org. Chem.*, **32**, 2506 (1967); (c) E. J. Fendler, J. H. Fendler, W. E. Byrne, and C. E. Griffin, *ibid.*, **33**, 4141 (1968).

7a. The stoichiometry of the stage I reaction (*vide infra*) indicates the spectrum to be due largely to 7a. σ-Complex formation at the 1 position is analogous to the complexing of $NaOCH_3$ with DNN methyl ether and is in harmony with the general proclivity of naphthalene derivatives with activating substituents in the 2 and 4 positions to undergo substitution at the 1 position.[12]

In this system, two rates are measurable (those of the stage I and stage II reactions) and two equilibria. The measurable equilibria are those between reactants and intermediate 7a (the stage I equilibrium) and between product 8a and its conjugate base 9a (the product equilibrium). Qualitatively, the system is the same with *t*-butylamine as with *n*-butylamine, but there are superficial differences which stem from differing magnitudes of rate and equilibrium constants.

Early in this investigation it became evident that the conjugate acid of the amine has a substantial effect on the stage II rate and on both equilibria. A known concentration of the relevant amine hydrochloride, frequently 0.01 *M*, was therefore established in most experiments. In all experiments, the amine was present in great excess over the substrate, and clean pseudo-first-order kinetics were observed.[13]

A Model for the System. Let us rewrite Scheme I in a fashion more useful for quantitative discussions as Scheme II. Equations 4 and 6 pertain to proton

Scheme II

$$5 + RNH_2 \underset{k_{-1}}{\overset{k_1}{\rightleftarrows}} 6 \quad (3)$$

$$6 + RNH_2 \overset{K_e}{\rightleftarrows} 7 + RNH_3^+ \quad (4)$$

$$7 + RNH_3^+ \overset{k_4}{\longrightarrow} 8 + C_2H_5OH + RNH_2 \quad (5)$$

$$8 + RNH_2 \overset{K_p}{\rightleftarrows} 9 + RNH_3^+ \quad (6)$$

transfer equilibria which are established rapidly. The stage I reaction (**5** $\rightleftarrows$ **7**) is much faster than the stage II reaction (**7** $\rightarrow$ **8**), and therefore the stage I reaction can be dealt with as an equilibrium. The stage I equilibrium constant (for the sum of eq 3 and 4) can be measured, and the rate of establishment of equilibrium can be resolved into components for the forward and reverse reactions. In the special case, often encountered with *n*-butylamine, in which the stage I equilibrium lies almost entirely on the right, the rate of the stage I reaction can be dealt with as though the reaction were irreversible.

As to the rate of the stage II reaction, the most general expression derivable from the model of Scheme II takes account of the possibility that the substrate may be split, in the stage I equilibrium, between **5** and **7**. Letting $[5]_{st} = [5] + [7]$, and letting K_i be the equilibrium constant for the stage I reaction, one derives

$$\text{rate} = k_{obsd}[5]_{st} = \frac{k_4K_i[RNH_2]^2[RNH_3^+][5]_{st}}{K_i[RNH_2]^2 + [RNH_3^+]} \quad (7)$$

(12) (a) N. McLeish and N. Campbell, *J. Chem. Soc.*, 1103 (1937); (b) L. F. Fieser in "Organic Chemistry, an Advanced Treatise," Vol. I, H. Gilman, Ed., John Wiley & Sons, Inc., New York, N. Y., 1943, Chapter 3.

(13) k_ψ symbolizes the pseudo-first-order rate coefficient for the stage I reaction, and k_{obsd} that for the stage II or overall reaction.

Cancelling, rearranging, and taking logarithms

$$\log k_{obsd} + \log (K_i[RNH_2]^2 + [RNH_3^+]) = \log k_4K_i + 2 \log [RNH_2] + \log [RNH_3^+] \quad (8)$$

In the special case in which $K_i[RNH_2]^2 \gg [RNH_3^+]$, that is, in which the stage I equilibrium lies almost wholly to the right, eq 7 simplifies to

$$k_{obsd} = k_4[RNH_3^+] \quad (9)$$

Reaction with *n*-Butylamine. Rate of Stage I, Forward. Under conditions of high amine concentration and low *n*-butylammonium ion concentration, the stage I equilibrium lies almost entirely to the right and the stage II reaction is relatively slow. The "infinity" absorbance represents virtually complete conversion to 7a, and it does not decay appreciably the time scale of the stage I reaction. The pseudo-first-order rate coefficient for the stage I reaction, forward, is then obtained simply as the slope of a plot of ln $(A_\infty - A_t)$ *vs.* time. In Table I, data collected under such conditions are assembled.

Table I. Reaction of **5** with *n*-Butylamine in DMSO. Stage I Reaction, Forward Rate[a]

Temp, °C	$[C_4H_9NH_2]$, *M*	$[C_4H_9NH_3Cl]$, *M*	$[(C_3H_7)_4NI]$, *M*	k_ψ, sec^{-1}	k_1,[b] M^{-1} sec^{-1}
		Part A			
25.4	0.045	0.010		1.51	33.6
	0.10	0.010		3.21	32.1
	0.20	0.010		6.29	31.5
	0.294	0.010		9.26	31.5
		Part B			
25.2	0.090	0		3.09	34.3
	0.090	0.0025		2.78	30.9
	0.090	0.0050		2.72	30.2
	0.090	0.010		2.84	31.5
	0.090	0	0.0025	2.77	30.8
	0.090	0	0.0050	2.74	30.4
	0.090	0	0.010	2.79	31.0
		Part C			
20.4	0.097	0.010		2.72	28.0
25.4	0.097	0.010		3.26	33.6
29.8	0.097	0.010		4.10	42.2
34.9	0.097	0.010		4.43	45.7

[a] $[Substrate]_0$ *ca.* 1×10^{-5} *M*; all k_ψ are average of duplicate runs; measurements at 527 nm. [b] $k_1 = k_\psi/[C_4H_9NH_2]$.

In Part A of Table I, amine concentration is varied while *n*-butylammonium chloride concentration is held constant. k_ψ[13] increases with amine concentration, but the quotient, $k_\psi/[C_4H_9NH_2]$, remains substantially constant. Thus the stage I reaction is first order in amine. In Part B, amine concentration is constant; the fact that k_ψ is unaffected by changes in *n*-butylammonium chloride and tetrapropylammonium iodide concentration shows that none of these ions appears in the rate law and that their salt effects are negligible within the range of salt concentrations studied. Part C concerns dependence of rate on temperature.

Stage I Equilibrium. Only at very low amine and substantial *n*-butylammonium ion concentrations does this equilibrium lie sufficiently in the middle for a good estimate of the equilibrium constant to be made. Knowing the extinction coefficient for 7a as measured under

Table II. Reaction of **5** with *n*-Butylamine in DMSO. Experiments to Determine the Stage I Equilibrium Constant

Temp, °C	$[C_4H_9NH_2]$, *M*	$[C_4H_9NH_3Cl]$, *M*	A_{527},[a] method A	K_i, method A, M^{-1}	A_{527},[a] method B	K_i method B, M^{-1}	k_{obsd},[b] sec^{-1}	K_i, method C, M^{-1}
			Part A					
18.8	1.94×10^{-3}	5.0×10^{-3}	0.110	1110				
24.2	1.94×10^{-3}	5.0×10^{-3}	0.075	600				
29.0	1.94×10^{-3}	5.0×10^{-3}	0.054	382				
31.6	1.94×10^{-3}	5.0×10^{-3}	0.043	287				
31.6	>0.2	1.0×10^{-2}	0.242	[c]				
33.7	1.94×10^{-3}	5.0×10^{-3}	0.035	224				
			Part B					
25.4	1.6×10^{-3}	1.0×10^{-2}			0.102	537	0.012	550
25.4	3.2×10^{-3}	1.0×10^{-2}			0.282	500	0.033	480
25.4	4.8×10^{-3}	1.0×10^{-2}			0.490	560	0.054	510
25.4	6.4×10^{-3}	1.0×10^{-2}			0.61	676	0.064	430
25.4	2.0×10^{-2}	1.0×10^{-2}			[d]		0.096	
25.4	4.0×10^{-1}	0			0.828			
			Part C					
25.4	4.76×10^{-3}	2.5×10^{-3} [e]			0.667	600	0.025	
25.4	4.76×10^{-3}	5.0×10^{-3} [f]			0.565	560	0.038	540
25.4	4.76×10^{-3}	1.0×10^{-2}			0.433	535	0.052	490

[a] See text regarding methods used to evaluate A_{527} (the absorbance at 527 nm at conclusion of stage I reaction but before appreciable stage II reaction had occurred). [b] See ref 13; the data listed are averages of (concording) values determined from the decrease in absorbance at 527 nm (on the time scale of the stage II reaction) and the increase in absorbance at 392 nm. [c] At the high $[C_4H_9NH_2]$ of this experiment, no estimate of K_i could be made. [d] Not recorded. [e] $(n\text{-}C_3H_7)_4N^+I^-$, 7.5×10^{-3} *M*, also present. [f] $(n\text{-}C_3H_7)_4N^+I^-$, 5.0×10^{-3} *M*, also present.

conditions where the equilibrium lies almost wholly to the right, one would expect to be able to estimate from the absorbance at 527 nm (λ_{max} for **7a**) the extent to which **7a** has been formed and straightforwardly to calculate the equilibrium constant. However, the conditions under which the equilibrium does not lie overwhelmingly on the side of **7a** are also conditions in which the stage II reaction rate approaches the stage I rate. The stage I "infinity" absorbance is not always sufficiently stable for the stage I equilibrium constant to be reckoned directly from it.

We used three methods to deal with this awkward situation. The first used data obtained from study of the stage I reaction in the stopped-flow apparatus. The apparent "infinity" absorbance at 527 nm (*i.e.*, the absorbance at approximately ten half-lives) was used to construct a plot of $\ln (A_\infty - A_t)$ *vs.* time; if the plot was not linear, "A_∞" was adjusted by small increments or decrements until a linear plot was obtained, and the value which afforded a linear plot was taken to be the proper stage I infinity absorbance. We call this method A.

The second method (B) used data obtained from kinetic study of the stage II reaction. The linear plots of $\log (A_t - A_\infty)$ against time were extrapolated back to zero time (time of addition of substrate) and A_0 was calculated from the intercept. A problem with this method is that the time of addition of substrate is not the proper zero time, because the time required to establish the stage I equilibrium is not negligible.

The third method (C) is kinetic. Rate coefficient k_1 is estimated from measurements under conditions suitable for utilization of eq 9. Then from other measurements, under conditions which require the full eq 7, k_{obsd} is determined at known $[RNH_2]$ and $[RNH_3^+]$, and K_i is calculated.

Results obtained by the three methods are set forth in Table II. For the determinations at 25.4°, the average value for K_i by method B is 570 M^{-1} and by method C 500 M^{-1}. These values bracket the value of K_i at 25.4° as determined by method A (interpolated in Part A, Table II), namely, 543 M^{-1}.

The K_i values in Table II were all reckoned on the basis of eq 10, that is, for equilibrium between **5** and **7a** in accordance with eq 3 and 4. It is to be noted that K_i remains substantially constant over a 12-fold

$$K_i = \frac{[7][RNH_3^+]}{[5][RNH_2]^2} \qquad (10)$$

variation in $[C_4H_9NH_2]$, while $[C_4H_9NH_3^+]$ is constant (Table II, Part B), and over a 4-fold variation in *n*-butylammonium ion concentration while amine concentration is constant (Part C). A trial assumption was made to the effect that the equilibrium under study was that of eq 3 (without eq 4), but equilibrium "constants" computed on the basis of that assumption ranged from 88 to 4330 M^{-1}.

The fact that eq 10 prevails shows that the intermediate complex exists predominantly as its conjugate base (**7a**) rather than its neutral, zwitterionic form (**6a**), as often written in earlier discussions. This is consistent with the stoichiometry established by Crampton and Gold[14] for the complexing of 1,3,5-trinitrobenzene with primary and secondary aliphatic amines in DMSO; two molecules of amine react with one of trinitrobenzene to form the conjugate base of the inital σ complex and an alkylammonium ion. Bernasconi[15] has evidence for the same stoichiometry for reactions of the same type in water solution.

Rate of Stage II. Under all the conditions used in this study, the rate of overall reaction to form final product **8a** (or **9a**) is controlled by the rate of the stage II reaction. In Figure 2, the overall pseudo-first-order rate coefficient at constant (0.01 *M*) concentration of

(14) M. R. Crampton and V. Gold, *J. Chem. Soc., B*, 23 (1967).
(15) C. F. Bernasconi, personal communication.

Table III. Reaction of **5** with *n*-Butylamine in DMSO. Stage II Reaction[a]

Temp, °C	$[C_4H_9NH_2]$, *M*	$[C_4H_9NH_3^+Cl^-]$, *M*	$[Pr_4N^+I^-]$, *M*	10^2k_{obsd}, sec^{-1}	k_4,[b] M^{-1} sec^{-1}
		Part A			
25.4	0.366	0	0.010	0.14	
	0.366	0.0020	0.0080	2.51	12.5
	0.366	0.0040	0.0060	4.55	11.4
	0.366	0.0060	0.0040	6.37	10.6
	0.366	0.0080	0.0020	8.03	10.0
	0.366	0.010	0	9.78	9.8
		Part B			
15.5	0.097	0.010	0	4.02	4.02
20.5	0.097	0.010	0	6.02	6.22
25.3	0.097	0.010	0	9.34	9.34
30.3	0.097	0.010	0	15.5	15.5
35.1	0.097	0.010	0	23.6	23.6

[a] $[Substrate]_0$ *ca.* 2.5×10^{-5} *M*; all k_{obsd} are averages of at least duplicate measurements at 392 nm. [b] $k_4 = k_{obsd}/[C_4H_9NH_3^+Cl^-]$.

Table IV. Determination of the Product Equilibrium Constant with *n*-Butylamine in DMSO

Temp, °C	$[n\text{-}BuNH_2]$, *M*	$[n\text{-}BuNH_3^+Cl^-]$, *M*	$[Pr_4N^+I^-]$, *M*	A_{524} nm[a]	K_p
			Part A[b]		
18.9	3.9×10^{-3}	6.0×10^{-3}	0	0.450	1.69
22.9	3.9×10^{-3}	6.0×10^{-3}	0	0.406	1.38
28.5	3.9×10^{-3}	6.0×10^{-3}	0	0.344	1.03
33.8	3.9×10^{-3}	6.0×10^{-3}	0	0.285	0.763
			Part B[c]		
25.4	1.6×10^{-3}	0.010	0	0.117	1.30
	3.2×10^{-3}	0.010	0	0.201	1.32
	4.8×10^{-3}	0.010	0	0.265	1.34
	6.4×10^{-3}	0.010	0	0.308	1.31
	2.0×10^{-2}	0.010	0	0.509	1.52
	3.0×10^{-2}	0.010	0	0.553	1.50
	4.0×10^{-2}	0.010	0	0.584	1.58
	0.40	0.010	0	0.676	
			Part C[d]		
25.4	4.76×10^{-3}	2.5×10^{-3}	7.5×10^{-3}	0.443 (0.449)	1.14 (1.09)
	4.76×10^{-3}	5.0×10^{-3}	5.0×10^{-3}	0.347 (0.355)	1.22 (1.21)
	4.76×10^{-3}	1.0×10^{-2}	0	0.250 (0.254)	1.33 (1.30)
	6.0×10^{-2}	0	0	0.646 (0.665)	

[a] A_{524nm} is the absorbance due to **9a** of the infinity solution of reaction of **5** with *n*-butylamine. [b] $[5]_0 = 3.3 \times 10^{-5}$ *M*, wavelength used was 527 nm. [c] $[5]_0 = 2.7 \times 10^{-5}$ *M*. [d] $[5]_0 = 2.64 \times 10^{-5}$ *M*. Numbers in brackets are values obtained using an authentic sample of product, **8a**, instead of infinity mixtures; $[8a]_0 = 2.67 \times 10^{-5}$ *M*.

n-butylammonium chloride is plotted as a function of *n*-butylamine concentration. The rate ascends steeply at low amine concentrations, but it is essentially constant at amine concentrations above 0.02 *M*. At 0.02 *M* and above, the stage I equilibrium lies almost wholly on the side of **7a**. It is apparent that the rate of conversion of **7a** to **8a** (or **9a**) is independent of amine concentration, at constant concentration of amine hydrochloride.

The ascending segment of the plot in Figure 2 occurs at amine concentrations at which the stage I equilibrium lies only partially on the side of **7a**; indeed, the data for the ascending segment are from experiments (Table II, Part B) which were used to evaluate K_i, the stage I equilibrium constant. In the ascending segment, the increase in k_{obsd} parallels the increase in concentration of intermediate complex **7a**.

The data in Table III, Part A, concern the dependence of the stage II rate on concentration of *n*-butylammonium chloride, at a constant amine concentration (0.366 *M*) which is sufficient to force the stage I equilibrium almost fully to the side of **7a**. In these experiments, total salt concentration is maintained constant by compensation with tetrapropylammonium iodide. It is evident that k_{obsd} increases steadily with *n*-butylammonium chloride concentration. The second-order rate coefficient k_4, reckoned as $k_{obsd}/[C_4H_9NH_3Cl]$

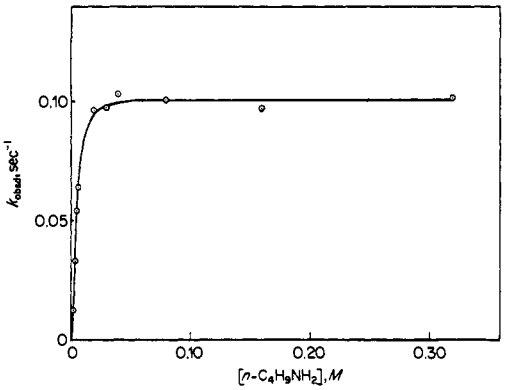

Figure 2. Rate coefficient for overall reaction of **5** with *n*-butylamine to form **8a** (or **9a**) as a function of amine concentration at constant (0.01 *M*) *n*-butylammonium chloride concentration. Points on the steep ascending segment are from Table II, Part B.

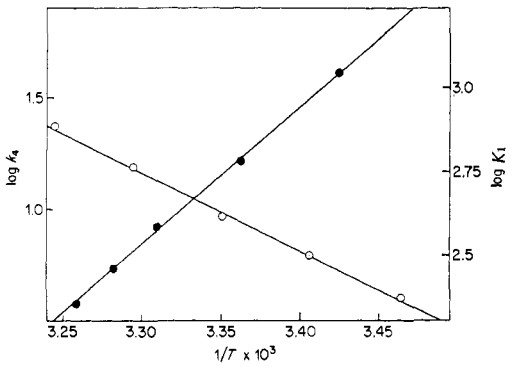

Figure 3. Arrhenius plot (open circles, left scale) based on k_4 values, and van't Hoff plot (filled circles, right scale) based on K_1 values, both for reaction of **5** with *n*-butylamine.

(see eq 9), is substantially constant. Thus, the conversion of intermediate complex **7a** to products is first order in *n*-butylammonium chloride concentration. The 20% decrease of k_4 between 0.002 *M* and 0.010 *M* amine hydrochloride is perhaps attributable to differential specific salt effects of this salt and tetrapropylammonium iodide.

The data of Table III, Part B, concern dependence of rate on temperature.

Product Equilibrium. Inasmuch as **8a** does not absorb but **9a** absorbs strongly at 524 nm, it is possible to determine the state of the acid–base equilibrium between **8a** and **9a** by photometric measurements at that wavelength, either on solutions prepared from isolated **8a** or on infinity solutions from kinetic determinations. Table IV summarizes a number of determinations of the equilibrium constant, K_p, defined as [**9a**][RNH_3^+]/[**8a**][RNH_2] (*cf.* eq 6). Most of the data of Table IV derive from measurements on infinity solutions. The experiments of Part A were performed especially to determine K_p, but those of Parts B and C concern experiments most of which appear also in Parts B and C, respectively, of Table II. However, the determinations of Table IV, Part C, were repeated under identical conditions with use of purified **8a**; the K_p values so obtained, enclosed in parentheses, are virtually the same as those based on kinetic infinity solutions.

In both Parts B and C of Table IV, the K_p values drift slightly with changing conditions. The drift in Part C resembles that in Table III, Part A, in the sense that *n*-butylammonium ion seems to lower the activity coefficient of an anionic species (**7a** or **9a**) selectively. A stabilizing hydrogen-bonding interaction is conceivable.

The possibility that the product equilibrium involves formation of a Jackson–Meisenheimer type σ-complex, rather than **9a**, was dismissed on the basis of an nmr experiment described in the Experimental Section.

Best Values and Derived Values. In Table V, we list best values for k_1, k_4, K_i, and K_p, as drawn from measurements presented above, for the standard temperature, 25.4°. Also listed is the quotient, k_{-1}/K_e, reckoned as k_1/K_i, pertaining to reversion of **7a** to **5** according to eq 3 and 4. Thermodynamic parameters and quasi-thermodynamic activation parameters, reckoned from the temperature dependence of equilibrium constants and rate coefficients, respectively, are

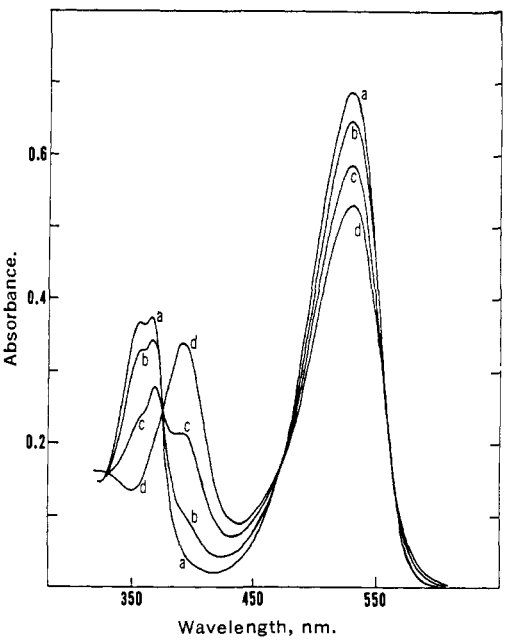

Figure 4. Spectra of mixtures of **5** and *t*-butylamine in DMSO solution at various times after mixing. Curves a, b, c, and d are for 9, 57, 224, and 2790 min, respectively.

also tabulated. Representative Arrhenius and van't Hoff plots are displayed in Figure 3. Practical considerations restricted measurements to a fairly narrow temperature range; the solvent freezes at 18.4°, and the greater temperature dependence of k_4 than of k_1 makes it difficult to obtain a good separation of stage I from stage II kinetics at higher temperatures.

Table V. Summary of Rate Coefficients, Equilibrium Constants, Thermodynamic and Activation Parameters

Reaction[a]	Parameter[b]	Reaction with *n*-butylamine[c]	Reaction with *t*-butylamine[c]
5 ⟶ **6**	k_1, M^{-1} sec^{-1}	31.8	0.51
	$\Delta G^{\ddagger}$	15.4	17.9
	$\Delta H^{\ddagger}$	5.8	
	$\Delta S^{\ddagger}$	−32	
5 ⇄ **7**	K_i, M^{-1}	540	0.074
	$\Delta G°$	−3.7	1.6
	$\Delta H°$	−19	
	$\Delta S°$	−51	
7 ⟶ **5**	k_{-1}/K_e, sec^{-1}	0.059	4.9
	$\Delta G^{\ddagger}$	19.1	16.5
	$\Delta H^{\ddagger}$	24.4	
	$\Delta S^{\ddagger}$	18	
7 ⟶ **8**	k_4, M^{-1} sec^{-1}	10.1	0.42
	$\Delta G^{\ddagger}$	16.1	18.0
	$\Delta H^{\ddagger}$	15.6	
	$\Delta S^{\ddagger}$	−2	
8 ⇄ **9**	K_p	1.35	0.056
	$\Delta G°$	−0.2	1.7
	$\Delta H°$	−9.2	
	$\Delta S°$	−30	

[a] See Scheme I. [b] Units of $\Delta G°$, $\Delta G^{\ddagger}$, $\Delta H°$, and $\Delta H^{\ddagger}$ are kilocalories per mole; units of $\Delta S°$ and $\Delta S^{\ddagger}$ are gibbs per mole. [c] Temperature 25.4° for *n*-butylamine, 25.0° for *t*-butylamine.

Reaction with *t*-Butylamine. General Features. In Figure 4, spectra of a mixture of **5** and *t*-butylamine in DMSO at various times after mixing are shown. The

Table VI. Reaction of **5** with *t*-Butylamine in DMSO. Stage I Equilibrium Constant and Rate Constants for Product Formation (Stage II)

Temp, °C	[*t*-$BuNH_2$], *M*	[*t*-$BuNH_3^+Cl^-$], *M*	[$Pr_4N^+I^-$], *M*	k_{obsd}, $sec^{-1} \times 10^4$	A_i[a]	K_i, M^{-1}	k_4,[b] $M^{-1}\ sec^{-1}$
			Part A[c]				
25.0	0.097	0.010	0	2.96	0.055	0.079	0.43
	0.145	0.010	0	6.18	0.112	0.079	0.44
	0.194	0.010	0	9.20	0.175	0.075	0.52
	0.291	0.010	0	16.6	0.320	0.080	0.41
	0.388	0.010	0	21.3	0.405	0.070	0.42
	0.485	0.010	0	25.0	0.475	0.064	0.42
	0.679	0.010	0	30.4	0.600	0.068	0.40
	0.97	0	0		0.792		
			Part B[d]				
25.4	0.82	0	0.050	2.90	0.760		
	0.82	0.0010	0.049	6.42	0.753		
	0.82	0.0030	0.047	12.6	0.724	0.091	0.338
	0.82	0.0070	0.043	22.2	0.695	0.112	0.302
	0.82	0.020	0.030	42.8	0.613	0.124	0.249
	0.82	0.050	0	71.7	0.493	0.137	0.213

[a] Stage I infinity reading 532 nm. [b] Calculated using a rearranged form of eq 8 (text). [c] $[Substrate]_0 = 2.56 \times 10^{-5}$ *M*. Values are results of single determinations except at [*t*-$C_4H_9NH_2$] = 0.679, which are averages of three runs. [d] $[Substrate]_0 = 2.45 \times 10^{-5}$ *M*. All values are averages of duplicate runs.

similarity to the corresponding curves from *n*-butylamine (Figure 1) is noteworthy. The spectral changes are interpreted as with *n*-butylamine. The intermediate (**7b**) has λ_{max} at 532 nm (ϵ 31,000), 368 nm, and 360 nm.

In the reaction of **5** with *t*-butylamine, the stage I equilibrium does not lie sufficiently on the side of **7b**, at appreciable concentrations of *t*-butylammonium chloride, for the stage I and stage II kinetics to be dealt with by the simple methods used with *n*-butylamine. The methods used are, however, fully rigorous.

Stage I Equilibrium. The data in Table VI, Part A, in the column headed A_i show that increasing *t*-butylamine concentration increases the amount of intermediate complex **7b** formed in the stage I equilibrium, at constant concentration of the amine hydrochloride. The data in the same column, Part B, demonstrate that at constant amine concentration the amount of **7b** formed is diminished by increasing the *t*-butylammonium chloride concentration. K_i, computed according to eq 10, is substantially constant within Part A but varies somewhat within the experiments of Part B. The constancy of K_i in Part A and the near constancy in Part B, despite a 17-fold variation in [*t*-$C_4H_9NH_3Cl$], indicate that eq 10 is appropriate and that the intermediate observed is **7b** rather than **6b**. The variation of K_i within Part B and the fact that an interpolated K_i in Part B at 0.010 *M* *t*-butylammonium chloride, namely, 0.115 M^{-1}, is rather greater than the K_i's in Part A indicate that both *t*-butylammonium chloride and tetrapropylammonium iodide (the compensating salt in Part B) exert salt effects on the equilibrium.

Stage I Kinetics. Because K_i is so low in the *t*-butylamine reaction, the forward rate could not be determined in isolation (as with *n*-butylamine) at moderate concentrations of the amine and amine hydrochloride. However, it could be determined as a component of the rate of establishment of the stage I equilibrium. k_ψ[13] for the attainment of equilibrium, measured by the stopped-flow photometric method, are presented in Table VII.

The pseudo-first-order rate coefficient for the attainment of equilibrium is the sum of the pseudo-first-order coefficients for the forward and reverse reactions. Therefore, eq 11 applies; *cf.* eq 3 and 4

$$k_\psi = k_1[RNH_2] + \frac{k_{-1}[RNH_3^+]}{K_e[RNH_2]} \quad (11)$$

Multiplying each side by $[RNH_2]$

$$k_\psi[RNH_2] = k_1[RNH_2]^2 + (k_{-1}/K_e)[RNH_3^+] \quad (12)$$

In accordance with eq 12, a plot of k_ψ[*t*-$C_4H_9NH_2$] (from Table VII) against [*t*-$C_4H_9NH_2$]^2 is linear; see Figure 5. The slope, k_1, is 0.51 $M^{-1}\ sec^{-1}$. This compares favorably with k_1 as determined directly in the absence of amine hydrochloride, conditions under which the equilibrium lies almost entirely on the right and k_ψ is virtually equal to $k_1[RNH_2]$; the last experiment of Table VII and footnote *c* of Table VII are relevant; they lead to an estimate of k_1 of 0.46 $M^{-1}\ sec^{-1}$. The intercept in Figure 5 is 0.049 *M* sec^{-1} and, from eq 12, k_{-1}/K_e is 4.9 sec^{-1}.

The quotient, $k_1/(k_{-1}/K_e)$, should equal K_i, the stage I equilibrium constant. From the data of Table VII and Figure 5, K_i is so estimated as 0.104 M^{-1}. This is somewhat higher than the K_i of 0.074 M^{-1} obtained from the data of Table VI, Part A, but agrees rather well with the data of Table VI, Part **B**.

Stage II Kinetics. For reasons discussed above, it was necessary to use a more sophisticated treatment of experimental data than was necessary with *n*-butyl-

Table VII. Rate Coefficients for Establishment of Equilibrium in the Stage I Reaction of *t*-Butylamine with **5** in DMSO[a]

[*t*-$C_4H_9NH_2$], *M*	k_ψ, sec^{-1} [b]
0.0965	0.487
0.185	0.344
0.268	0.336
0.372	0.341
0.45	0.341
0.57	0.370
0.65	0.412
0.38[c]	0.175

[a] $[\mathbf{5}]_0$, 0.9×10^{-5} *M*; [*t*-$C_4H_9NH_3Cl$], 0.010 *M*; temperature, 25.0°. [b] Average values of duplicate or triplicate determinations. [c] No added *t*-$C_4H_9NH_3Cl$; $k_1 = 0.175/0.38 = 0.46\ M^{-1}\ sec^{-1}$.

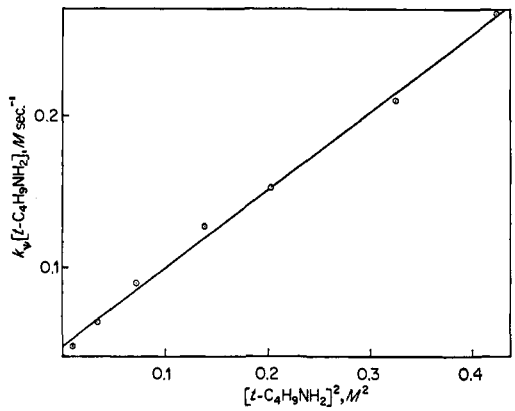

Figure 5. Stage I reaction of **5** with *t*-butylamine; plot according to eq 12; data from Table VII.

amine. Pseudo-first-order rate coefficients, k_{obsd}, for the overall reaction after the stage I equilibrium had been established were determined in two series of experiments which are summarized in Table VI. In one series (Part A), *t*-butylamine concentration was varied as *t*-butylammonium chloride concentration was held constant, and in the other series (Part B), *vice versa*. Both series are suitable for employment of eq 8.

Plots of the quantity on the left side of eq 8 against log $[t\text{-}C_4H_9NH_2]$ for the data of Part A and against log $[t\text{-}C_4H_9NH_3Cl]$ for the data of Part B were linear with slopes 1.9 and 0.86, respectively. These are presented in Figure 6. By means of eq 8, k_4 was then reckoned for each point; the values so obtained are listed in the last column of Table VI. The k_4 values in Part A are fairly constant, but those in Part B show a trend and are somewhat lower than those of Part A, probably because of kinetic salt effects.[16] We take the best value of k_4 to be 0.42 M^{-1} sec^{-1}.

Product Equilibrium. As discussed for *n*-butylamine, K_p for equilibrium between **8b** and **9b**, according to eq 6, may be estimated from the infinity absorbances from kinetic experiments. Table VIII presents relevant

Table VIII. Determination of the Product Equilibrium Constant with *t*-Butylamine in DMSO at 25.0° [a]

$[t\text{-}C_4H_9NH_2]$, M	$A_{532\ nm}$	K_p
0.097	0.252	0.066
0.145	0.296	0.060
0.194	0.342	0.060
0.291	0.398	0.058
0.388	0.422	0.051
0.485	0.442	0.047
0.679	0.495[b]	0.054[b]
0.97[c]	0.634	

[a] These are the same experiments as in Table VI, Part A. [b] Average of three determinations; the others are single runs. [c] No $t\text{-}C_4H_9NH_3Cl$ present.

data, pertaining to the same experiments as in Table VI, Part A. Measurements were made at 532 nm, λ_{max} for **9b**. The several estimates of K_p in Table VIII are in harmony with one another; the average value is 0.056.

(16) The appreciable rate observed in the first experiment of Table VI, Part B, suggests an uncatalyzed conversion of **7b** to **8b**. In contrast, the first experiment in Table III, Part A, shows a very low rate.

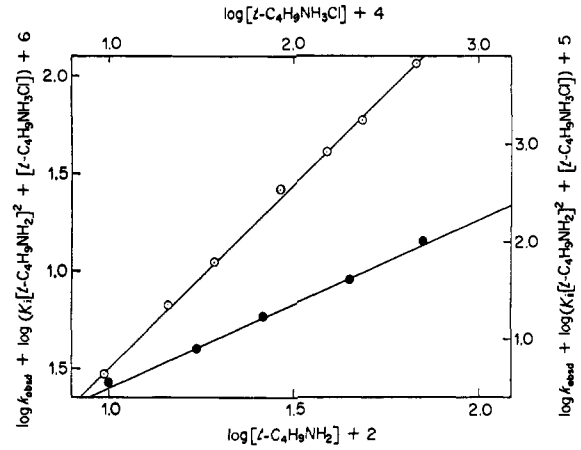

Figure 6. Overall reaction of **5** with *t*-butylamine; plots according to eq 8: open circles (left and bottom scales) are data of Table VI, Part A; filled circles (right and top scales) are data of Table VI, Part B.

Best Values and Derived Values. These are listed in Table V, alongside the corresponding values for *n*-butylamine. For *t*-butylamine, temperature dependence of rate coefficients and equilibrium constants was not determined, and thus enthalpies and entropies of reaction or activation cannot be calculated.

Discussion

The experimental evidence strongly supports representation of the reaction as in Schemes I and II.

The Intermediate Complex. The fact that the overall reaction occurs in two distinct stages is apparent in Figures 1 and 4; in both cases, curve a closely approximates the spectrum of the intermediate. The composition of the intermediate is demonstrated to be that of **7** (Scheme I) by the fact that the stage I equilibrium conforms to eq 10. The structure of the intermediate is indicated to be that of **7** by the similarity of its spectrum to that of an authentic Jackson–Meisenheimer σ complex of similar structure (Figure 1), by the slowness of its formation (which excludes the possibility that the intermediate is a charge transfer complex[17]), and by analogy with known activation and orientation patterns in reactions of naphthalene derivatives.[12]

The intermediate complex mechanism of aromatic nucleophilic substitution was already strongly indicated by evidence from steady-state kinetics and other sources. Direct observation of the intermediate further reinforces the case for this mechanism. It is to be noted, however, that demonstration of the transient formation of a species of structure **7** does not of itself prove this species to be an intermediate; it might represent the end of a cul-de-sac in the overall reaction scheme, the actual substitution occurring by some other route. It is the combination of this direct observation with kinetic and other evidence which makes the case for the intermediate complex mechanism a compelling one.

Demonstration that the predominant form of the intermediate complex is **7** rather than **6** under the conditions of our experiments is novel, although this might have been anticipated from knowledge of the stoichiometry of Jackson–Meisenheimer complex formation with

(17) J. E. Anderson and C. P. Smyth, *J. Amer. Chem. Soc.*, **85**, 2904 (1963).

amine nucleophiles.[14,15] It is probable that analogous intermediate complexes (*e.g.*, from 2,4-dinitrophenyl ethers) in protic solvents exist principally in the conjugate base form (**4**) rather than as the original σ complex (**2**) when they are formed in the presence of bases as strong as aliphatic amines.

Mechanism of the Stage I Reaction. The stage I rate law (first order in substrate, first order in amine) shows that only one amine molecule is involved in the rate-limiting transition state, and therefore that formation of the intermediate complex is not base catalyzed. The same conclusion was previously drawn from steady-state kinetics studies in related systems.[2,3]

The fact that the stage I rate law involves only one molecule of amine whereas the stoichiometry of formation of intermediate **7** involves two molecules of amine shows that there is an intermediate between **5** and **7**.[18] The intermediate undoubtedly has structure **6**.

Mechanism of the Stage II Reaction. In the introductory statement, we discussed three mechanisms, a, b, and c, which have been proposed to account for base catalysis of the transformation of an intermediate complex such as **2** to ultimate substitution products. As mentioned, there are already grounds for rejection of possibility a, that a proton transfer which converts **2** to **4** is rate limiting. Were mechanism a to prevail, the conjugate base intermediate complex (**4**) would necessarily decompose very rapidly to ultimate products. Our demonstration that intermediates **7a** and **7b** have half-lives of several minutes constitutes further compelling evidence against possibility a.

The present stage II kinetic data show that the transition state is composed of **7** plus one butylammonium ion. However, the kinetic data do not indicate how **7** and the butylammonium ion interact with each other. If mechanism c obtains, involving general acid catalysis of leaving group expulsion, **7** and the butylammonium ion interact in the sense of the transition state indicated in eq 2b. Such an interaction assigns a logical function to the butylammonium ion.[19]

If mechanism b, the E2-like mechanism, were to obtain, transformation of **7** to **8** would entail two steps: transfer of a proton from the butylammonium ion to the amino nitrogen of **7**, regenerating **6** and an amine molecule, and then return attack of the amine on the same proton to remove it with concerted departure of the ethoxy group as ethoxide ion. The transition state would be depicted as **10**. However, such a mechanism assigns no logical function to the butylammonium ion in transformation of **7** to **8**. Indeed, involvement of a butylammonium ion in the sense of transition state **10** should *retard* expulsion of the ethoxy group. Let us consider the probable relative free energies of **10** and of **11**, the latter being the transition state for direct expulsion of ethoxide ion from **7**. Transition states such as **11** are involved in lyate ion-catalyzed aminodealkoxylation reactions.

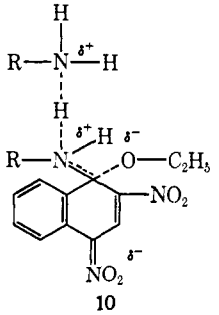

10

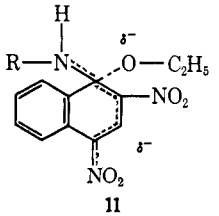

11

11 should have lower free energy than **10** both for entropic and enthalpic reasons. Because **10** incorporates a butylammonium ion which **11** does not, its entropy is depressed by roughly the translational and rotational entropy of the butylammonium ion, perhaps 15 to 20 gibbs/mol.[20] And because the valence electrons of the amino nitrogen nearer the ring in **10** are partially localized by the departing proton, the enthalpy of **10** should be greater.[21] We conclude that E2-like mechanism b for transformation of **7** to **8** is so unlikely, in view of the present experimental evidence, as not to warrant further advocacy unless new evidence specifically requiring it can be found.

Thus mechanism c, general acid catalyzed leaving group expulsion from the intermediate complex conjugate base, is strongly indicated.

Kinetic Expression for Base-Catalyzed Aminodealkoxylation Reactions. In most discussions these reactions have been represented as in eq 1, although the possibility that the predominant form of the intermediate may be its conjugate base (**4**) has been recognized.[2c,d,3] With attention to eq 1, the second-order rate coefficient k_A, defined as (d[product]/dt)/[ArX][R_2NH]), has usually been expressed as in eq 13 to

$$k_A = \frac{k_1(k_2 + k_3[B])}{k_{-1} + k_2 + k_3[B]} \qquad (13)$$

account for catalysis by a base B. Now that we have strong evidence that the predominant form of the intermediate is **4** rather than **2**, we should modify eq 13. The appropriate modification is to replace each k_3 in eq 13 by the product k_4K_e, where K_e is the equilibrium constant of eq 2a (or eq 4) and k_4 is the rate coefficient for reaction 2b (or 5).[2c,d] The modified expression is

$$k_A = \frac{k_1(k_2 + k_4K_e[B])}{k_{-1} + k_2 + k_4K_e[B]} \qquad (14)$$

Equation 14 emerges from a straightforward steady-state derivation if reaction 2a is considered to be a mobile equilibrium and the rate of formation of total intermediate (**2** plus **4**) is assumed equal to its rate of destruction.

A further consideration is that the uncatalyzed (k_2) term in eq 14 might represent either direct expulsion of X or HX from **2** or lyonium ion catalyzed expulsion of X from **4**. If the rate coefficient for the latter is k_2', each k_2 in eq 14 should be replaced by ($k_2 + k_2'K_a$), where K_a is the acid dissociation constant of **2**. One cannot tell from steady-state kinetics whether the k_2 or the $k_2'K_a$ term is the more important.

(18) J. O. Edwards, E. F. Greene, and J. Ross, *J. Chem. Educ.*, **45**, 381 (1968).

(19) C. A. Bunton and R. H. De Wolfe, *J. Org. Chem.*, **30**, 1371 (1965); W. P. Jencks, "Catalysis in Chemistry and Enzymology," McGraw-Hill Book Co., Inc., New York, N. Y., 1969, Chapter 10.

(20) K. B. Wiberg, "Physical Organic Chemistry," John Wiley & Sons, Inc., New York, N. Y., 1964, p 387; T. C. Bruice and S. J. Benkovic, *J. Amer. Chem. Soc.*, **86**, 418 (1964).

(21) Similar arguments pertain to the question of whether, in β elimination to form olefins, observation of exchange of β-hydrogens with the solvent constitutes evidence for the carbanion or Elcb mechanism; *cf.* J. F. Bunnett, *Survey Progr. Chem.*, **5**, 53 (1969).

Comparisons of Reactivity. Table V shows that *n*-butylamine exceeds *t*-butylamine in k_1 by about 60-fold and in K_i by about 7000-fold. The lower reactivity of *t*-butylamine is doubtless due to its bulkiness about nitrogen, which causes increased steric compressions in the stage I transition state (for reaction 3) and in intermediate **7b**. From the relative magnitudes of k_1 and K_i, and on the assumption that proton transfer equilibrium 4 is insensitive to the steric factor, one deduces that steric compressions are much more severe in intermediate **6b** than in the transition state leading to it. If the nucleophile initially attacks perpendicular to the plane of the aromatic ring, as is generally considered to be the case, the *t*-butyl group should have less interaction with the aromatic framework in the transition state than in the intermediate.

The 60-fold decrease in k_1, between *n*- and *t*-butylamine, compares with the 240-fold decrease reported for reactions of these amines with 2,4-dinitrochlorobenzene in benzene solvent.[22] There is evidence that amine attack is rate determining in the latter reactions. The rather modest difference between the amine structure effects in the two systems may be due to differing degrees of C–N bond formation at the transition state, or to the difference in solvents.

For the stage II reaction, the k_4 values show that reactivity is again greater in the *n*-butyl series, by about 25-fold. Two explanations are conceivable; there may be steric diminution of the effectiveness of the *t*-butylammonium ion as a general acid catalyst,[23] and/or steric compressions between the *t*-butyl group and the aromatic framework (especially with the 2-nitro group and the *peri*-CH) may increase as **7b** is converted to **8b**.

The product equilibrium constant, K_p, is also greater in the *n*-butylamine reaction series, by about 25-fold (Table V). Inasmuch as the two butylamines are nearly equal in basicity, the difference in K_p's indicates that steric compressions increase more (or decrease less) in going from **8b** to **9b** than in going from **8a** to **9a**. In **9a** or **9b**, the carbon of the butyl group which is attached to nitrogen must lie in the plane of the aromatic ring if the negative charge is effectively to be delocalized into the nitro groups. The angle between the two C–N bonds is about 120°. Regardless of whether the *t*-butyl group lies to the side of the *peri*-CH or to the side of the 2-nitro group, it is involved in substantial compressions against other atoms.

Experimental Section

Materials. Dimethyl sulfoxide (Matheson Coleman and Bell) was refluxed over CaH_2 and distilled just prior to use. In some of the earlier work, DMSO was purified by fractional freezing. The two methods of purification gave rate and equilibrium results which were not appreciably different. *n*-Butylamine and *t*-butylamine (Eastman Kodak products) were purified by refluxing over sodium and distilling; *n*-butylamine, bp 77°; *t*-butylamine, bp 44° (both uncorrected). Both amines were stored over molecular sieves (Linde). With *t*-butylamine, the originally colorless distillation product took on a slight greenish tinge after several days on the shelf. This did not happen when it was stored in the dark under nitrogen. The hydrochloride salts of the amines were prepared by addition of the proper amount of concentrated hydrochloric acid to an ethanol solution of the amine, isolation of the precipitated white solid, and recrystallization. *t*-Butylamine hydrochloride was recrystallized from ethanol and *n*-butylamine hydrochloride was recrystallized from acetonitrile. Both salts were dried *in vacuo* over P_2O_5. 2,4-Dinitro-1-naphthyl ethyl ether, mp 90–91° (from ethanol),[24] was prepared by the action of sodium ethoxide on an ethanolic solution of 1-chloro-2,4-dinitronaphthalene (DNNCl) (Eastman Kodak). The substitution products N-*n*-butyl- and N-*t*-butyl-2,4-dinitro-1-naphthylamines, **8a** and **8b**, were prepared by the reactions of the respective butylamines with DNNCl in DMSO solution. After recrystallization from 95% ethanol, melting points were: **8a**, 90.5–91.0°; **8b**, 119.0–119.6°. *Anal.*[25] Calcd for $C_{14}H_{15}N_3O_4$: C, 58.12; H, 5.23. Found for **8a**: C, 57.90; H, 5.28. Found for **8b**: C, 57.93; H, 5.23.

Spectra of Reactants and Products. Standard solutions of various substances were prepared by dissolving a few milligrams, accurately weighed, in 10.00 ml of DMSO. An exact amount of the standard solution (usually 20 μl) was added to 3.00 ml of DMSO, containing any other desired solute, which previously had been pipetted into a cuvette, and the cuvette was stoppered and shaken. Spectra were recorded using a Cary Model-14 spectrophotometer. Extinction coefficients determined in this way were quite reproducible. Wavelengths of maximum absorption (in nm) and some of the associated molar extinction coefficients (ε) are as follows: **5** in DMSO, 358 (6200); **7a** in *ca.* 0.4 *M n*-butylamine in DMSO, 353, 365, and 527 (30,600); **7b** in *ca.* 0.9 *M t*-butylamine in DMSO, 360, 370, and 532 (31,000); **8a** in DMSO, 410 (17,100); **8b** in DMSO, 410 (11,700); **9a** in 0.4 *M n*-butylamine in DMSO, 392 and 524 (25,000); **9b** in *ca.* 1 *M t*-butylamine in DMSO, 395 and 532 (24,200).

Preparation and Nmr Evidence for the Jackson–Meisenheimer Complex of $NaOCH_3$; with DNN Methyl Ether. The preparation of the Jackson–Meisenheimer complex of potassium methoxide with DNN methyl ether has been reported by Fendler, *et al.*[10] The nmr spectrum of their material in DMSO-d_6 along with the results of ir (in Nujol) and visible (in CH_3OH) spectra, gave confirmation of the Jackson–Meisenheimer structure. Our synthesis of this complex utilized sodium methoxide in methanol as the only solvent. The red solid product was recrystallized from a benzene–acetonitrile mixture; it did not melt below 240°, but underwent an irreversible color change from red to orange at about 170–200°.[26] The nmr spectrum of the red complex salt in DMSO of ordinary isotopic abundance agreed in every observable aspect with that reported by Fendler, *et al.*[10,27] The visible spectrum of the complex in DMSO has λ_{max} at 505, 362, and 351 nm, and in methanol 500 and *ca.* 350 nm.

Evidence for the Structure of 9a. The nmr spectrum of a solution of **8** in DMSO-d_6 was recorded. Neat *n*-butylamine was added to the nmr tube in small increments and the nmr spectrum was recorded after each addition. The molar ratios of *n*-butylamine to **8a** (initial concentration of **8a** = 0.28 *M*) employed were 0.35, 1.0, and 3.0. The spectral changes produced in the aromatic proton region, although clearly indicative of a chemical change, were not diagnostic between the alternative chemical processes considered, *i.e.*, eq 6 and 15. However, a single feature of the spectral changes

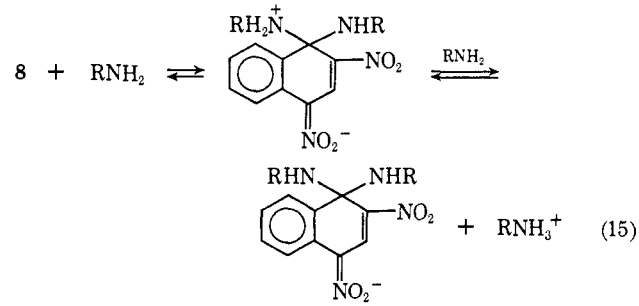

(15)

was sufficient to establish that eq 6 and not 15 is followed. In **8a**, the methylene protons of the carbon atom α to the amino nitrogen atom appear as a broadened triplet at 3.63 ppm (TMS internal

(22) F. Pietra and D. Vitali, *J. Chem. Soc., B*, 1200 (1968).
(23) *Cf.* F. Covitz and F. H. Westheimer, *J. Amer. Chem. Soc.*, **85**, 1773 (1963).
(24) P. Hiermann, *J. Prakt. Chem.*, **44**, 243 (1891), reported mp 93°.
(25) Analyses by Micro-Tech Laboratories, Inc., Skokie, Ill.
(26) The resulting orange solid was dissolved in water. On acidification of the solution, a yellow solid precipitated; it was identified as 2,4-dinitro-1-naphthol.
(27) In ordinary DMSO, the resonance position of the methyl protons of the complex anion and the strong absorption of the methyl protons of DMSO overlap somewhat.

standard). The aryl proton at the 3 position of the naphthalene moiety appears as a sharp singlet at 8.88 ppm. On addition of *n*-butylamine these peak positions change smoothly to 3.20 and 9.01 ppm, respectively, at the highest concentration of *n*-butylamine. Throughout this nearly ninefold change in the amount of *n*-butylamine added to the solution, and in spite of the large upfield shift of the α-methylene protons, the relative areas of the methylene proton triplet and the H-3 singlet remained constant at 2:1. This can only be consistent with eq 6 and not with 15, since in eq 15 this ratio of areas should increase as the equilibrium is shifted to the right.

Additional evidence for eq 6 lies in the fact that the stoichiometry established for the product equilibrium, K_p is that of eq 6, and is inconsistent with eq 15. If the reaction in eq 15 were primarily to the first complex (zwitterion), no dependence of K_p on *n*-butylammonium ion should have been found, and if the reaction were to the second complex, there should have been a square dependence on *n*-butylamine concentration.

Kinetic Procedures. Rates were measured photometrically by means of either conventional or stopped-flow technique. For the conventional technique, a Cary-14 spectrophotometer equipped with a special thermostated cell holder which maintained temperature constant within $\pm 0.02°$ was employed. Reaction solutions were prepared as follows: standard solutions of amine, amine hydrochloride, and tetrapropylammonium iodide in DMSO were prepared; for a given run, appropriate volumes of the appropriate solutions were combined and diluted quantitatively with DMSO at room temperature; 3.00 ml of the resulting solution was placed in a cuvette which was allowed to come to thermal equilibrium in the cell compartment; 20 μl of a standard solution of substrate was injected and mixed; and absorbance at the chosen wavelength was followed with time. For the stopped-flow technique, a Durrum–Gibson stopped-flow spectrophotometric apparatus was employed.

Acknowledgments. We are grateful to Professor C. F. Bernasconi for critical discussions and for information about experiments in progress and to Mrs. Carol Cornelson King for assistance with some of the experiments.

A Study of the Photolytic Stabilities of Fluoroalkyl Iodides by Electron Spin Resonance Trapping Techniques and the Temperature Dependence of the Nitroxide Splitting Constants

Kenneth J. Klabunde

Contribution from the Department of Chemistry, University of Iowa, Iowa City, Iowa 52240. *Received August 22, 1969*

Abstract: Radicals formed by the photolysis of fluoroalkyl iodides have been trapped with 2-nitroso-2-methylpropane (NOMP), and the resultant esr spectra have been analyzed. Relative photolytic stabilities of the iodides were determined by competitive photolysis and trapping experiments. The results show that the groups which allow facile radical formation are in the order $C_6H_5 > Cl \gtrsim CF_3CF_2 > CF_3 > F > H$. In addition, temperature studies with several of the trapped radicals have shown large changes in fluorine splitting constants. These changes can be rationalized in terms of preferred structural conformations at low temperatures as well as fluorine–nitrogen p–π interactions.

Several esr studies of chemically trapped short-lived free radicals have recently appeared.[1–7] Diphenylnitrone,[3] phenyl-*t*-butylnitrone (PBN),[3,5,6] and 2-nitroso-2-methylpropane (NOMP)[1,2,4] have been used successfully. The latter reagent has been employed for the study of radicals formed by photolysis,[1] polymerization,[4] and γ-ray bombardment.[2] In the present work NOMP was used to study the photochemical formation of fluorinated alkyl free radicals from fluoroalkyl iodides.

Recently, interest has grown in the elucidation of the effectiveness of through space fluorine p–π interactions (*cf.* Discussion) first invoked by Sheppard. Substituent effect studies have indicated that this interaction may be quite important.[8,9] However, initial opposition to this concept has helped to instigate additional work in the area.[10] Esr studies have been useful in this respect. Fluorinated aryl radical anions have shown temperature-dependent fluorine splittings which have been rationalized in terms of p–π interactions.[11,12] Fluorine–nitrogen p–π interactions have been indicated by esr studies. Strom and Bluhm[13] rationalized unusually large fluorine splittings using this interaction concept. Sheidler and Bolton[14] have presented some of the strongest evidence for fluorine–nitrogen p–π interactions. These workers found that

(1) A. Macker, Th. A. J. W. Wajer, Th. J. DeBoer, and J. D. W. vanVoorst, *Tetrahedron Lett.*, 2115 (1966).
(2) C. Lagercrantz and S. Forshult, *Nature*, **218**, 1247 (1968).
(3) M. Iwamura and N. Inamoto, *Bull. Chem. Soc. Jap.*, **40**, 702, 703 (1967).
(4) G. R. Chalfont, M. J. Perkins, and A. Horsfield, *J. Am. Chem. Soc.*, **90**, 7141 (1968).
(5) E. G. Janzen and B. J. Blackburn, *ibid.*, **90**, 5909 (1968); **91**, 4481 (1969).
(6) Janzen and Blackburn[5] have carefully characterized phenyl-*t*-butylnitrone (PBN) as a trapping agent. It has been pointed out, however, that PBN is not effective as a trap for large radicals such as heptafluoroisopropyl[7] and triphenylmethyl.[6] Also, PBN is slightly susceptible to photolysis itself, and in the present work it was found that the large fluoroalkyl radicals (formed from the photolysis of the corresponding iodides) were not trapped by PBN. Instead, the PBN broke down upon photolysis to yield a small amount of NOMP which trapped the fluoroalkyl radicals. Thus, nearly identical esr spectra were obtained by the photolysis of heptafluoroisopropyl iodide in the presence of PBN or in the presence of NOMP. (Diphenylnitrone was also found to decompose upon photolysis.)
(7) E. G. Janzen, private communication.
(8) W. A. Sheppard, *J. Am. Chem. Soc.*, **87**, 2410 (1965).
(9) W. A. Sheppard, *Trans. N. Y. Acad. Sci.*, (2) **29**, (6), 700 (1967).
(10) M. J. S. Dewar and A. P. Marchand, *J. Am. Chem. Soc.*, **88**, 354 (1966).
(11) J. C. Danner and A. H. Maki, *ibid.*, **88**, 4297 (1966).
(12) M. T. Jones, *J. Chem. Phys.*, **42**, 4054 (1965).
(13) E. T. Strom and A. H. Bluhm, *Chem. Commun.*, 115 (1966).
(14) P. J. Sheidler and J. Bolton, *J. Am. Chem. Soc.*, **88**, 371 (1966).